A Hydrophobic Antireflective and Antidust Coating With SiO_2 and TiO_2 Nanoparticles Using a New 3-D Printing Method for Photovoltaic Panels

Nazmi Ekren, Ali Samet Sarkin, and Şafak Sağlam

***Abstract*—The main outdoor factors that reduce the efficiency of the photovoltaic (PV) panel are the reflection and refraction of light, dirt, dust, and organic waste accumulating on the panel surface. In this article, an antireflection, self-cleaning coating was applied on the PV panel cover glass with a new method. With the coating, the surface has been given a hydrophobic feature. As a coating method, a 3-D printer has not been seen in the literature and used as a new method. The electrospinning method has also been tried as an alternative method. Solutions in different combinations were developed using polylactic acid or polymethylmethacrylate polymer, chloroform ($CHCl_3$) as a solvent, and silicon dioxide (SiO_2) and titanium dioxide (TiO_2) nanoparticles as primary materials in a modified 3-D printer for bioprinting. Five PV panels were obtained by applying different 3-D parameters from three solutions, which have the best results. Coating thicknesses are in the range of 3.12–8.47 μm. Coated and uncoated PV panels were tested in outdoor conditions for ten-day periods. The power outputs of the PV panels were measured, and their ten-day average efficiency was presented. According to the results, the highest efficiency increase is 8.7%. The highest light transmittance is 88.2% at 550 nm. In addition, hydrophobic properties were observed on all surfaces and the water contact angle was measured as 96.18°.**

***Index Terms*—3-D printing, antireflection, hydrophobic, nanoparticle, photovoltaic (PV), self-cleaning.**

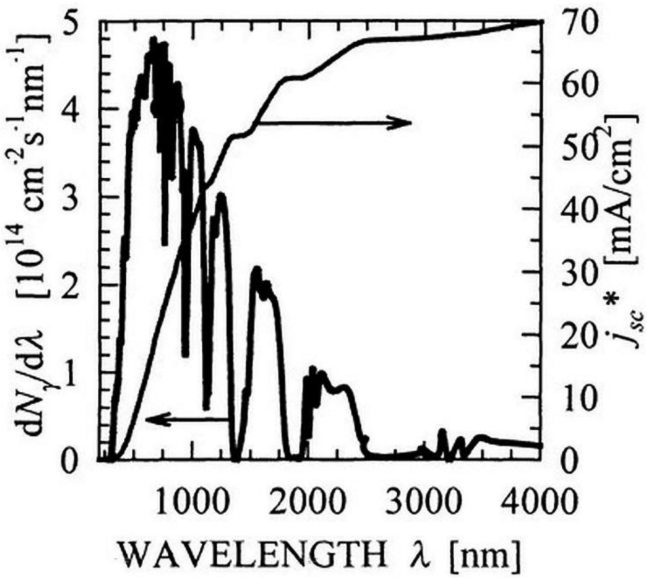

Fig. 1. Photon flux density(dN), wavelength (λ), and current density (J_{sc}) [2].

I. Introduction

DIFFERENT energy generation sources and technologies are used to meet the electrical energy demand in the world. It is aimed to reduce the use of fossil fuels due to toxic wastes, air pollution, damage to the ozone layer, and general climatic effects. Solar and wind power plants have become widespread with the support of renewable energy resources, replaced instead of fossil fuels, whose share in electrical energy consumption has been reduced.

In wind and solar power plants, issues, such as improvement and efficiency increase, have been studied for years. Electricity generation in solar power plants is commonly made in two different technologies: solar thermal known as concentrated solar power and photovoltaic (PV) systems [1]. Panel power output, open-circuit voltage, and short-circuit current are determined by the serial and parallel connection of the silicon cut cells in the solar panel.

In theory, PV cells have approximately 30% efficiency, open-circuit voltages (V_{oc}) 610–625 mV, and short-circuit currents (I_{sc}) 42 mA/cm^2 under 1.5 A.M. solar radiation [2]. In contrast to the theory, these values cannot be reached in practice today. In practice, the efficiency can be 24.3%, V_{oc} 600 mV, and I_{sc} 34 mA/cm^2 [3]. We can see the limitation of short-circuit currents (current density-J_{sc}) depending on the wavelength in Fig. 1. As the wavelength of the light increases, the more current density can be obtained, but due to the photon flux density, silicon cells are nominally effective in the wavelength range of 300–1100 nm [4]. This effect can be seen in Fig. 1 as photon flux density (dN).

The differences in theory and practice can be divided into optical losses and electrical (recombination and resistivity) losses [5]. Optical losses are based on reflection, refraction, and insufficient absorption of light. When the light comes to the

Manuscript received April 7, 2022; revised May 6, 2022; accepted May 16, 2022. Date of publication June 6, 2022; date of current version June 21, 2022. *(Corresponding author: Nazmi Ekren.)*

Nazmi Ekren and Şafak Sağlam are with the Electrical and Electronical Engineering Department, Marmara University, 34854 İstanbul, Türkiye (e-mail: nazmiekren@marmara.edu.tr; ssaglam@marmara.edu.tr).

Ali Samet Sarkin is with the Osmaniye Korkut Ata University, 80750 Osmaniye, Türkiye (e-mail: sametsarkin@osmaniye.edu.tr).

Color versions of one or more figures in this article are available at https://doi.org/10.1109/JPHOTOV.2022.3177229.

Digital Object Identifier 10.1109/JPHOTOV.2022.3177229

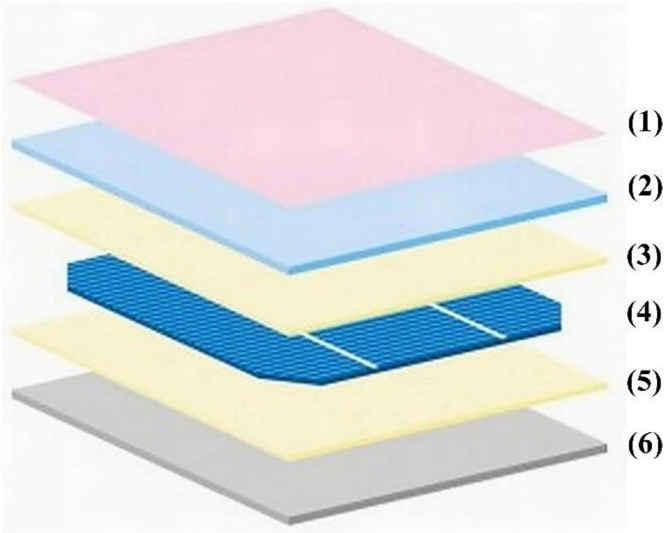

Fig. 2. PV panel(mono-c) components and ARC on cover glass [12].

cover glass surface of the PV solar panel, some of it refracts, then reaches the cell, and some of it reflects. The amount of light passing the silicon cell is 90% of the radiation intensity reaching the cover glass surface. A radiation loss of 10% is seen as a significant loss in total electrical energy production. In a PV panel, not only reflection but also pollution and dirt cause a reduction in electricity generation. Therefore, antireflective coating (ARC) and self-cleaning featured coating are made on the solar panel. While the coatings applied to the cell surface can only be antireflective, the coatings made on the PV panel glass can be antireflective and self-cleaning. Pure silicon wafer reflects 27.4%–35% of the light [6]–[8]. The reflection index of the air is "1.00," and the glass is "1.52," the mentioned loss of 10% occurs during the transition of photons from low index to high index [9], [10]. Because of this phenomenon, when coating the glass surfaces of PV panels, the reflection index of the ARC should be between the index of the air and the coated surface [11]. The components of the PV panels and the position of the ARC made on the cover glass are shown in Fig. 2.

It is necessary to consider antireflective and self-cleaning coatings as materials and methods. Coatings are made by sol-gel method with spin-coating or dip-coating applications, physical or chemical vapor deposition, sputtering, atomic layer deposition, screen printing, laser deposition, and spray coating methods [13]–[15]. These methods are the most common. Apart from these methods, electrospinning and electrospraying have been seen in the literature [16]. In addition, it has been seen in the literature that studies are using antireflective and self-cleaning materials together [17]. In terms of material, silicon dioxide (SiO_2) is the most used particle in ARCs in the literature due to its cost-effectiveness, ease to access, and reflection index of 1.46 [18], [19]. As an alternative to SiO_2, the most widely used material is MgF_2, with a reflection index of 1.32 [20].

In the literature, titanium dioxide (TiO_2) is the most widely used material in studies on self-cleaning coatings; as the wavelength (nm) increases, the photon density decreases. TiO_2 with a 3.2-eV bandgap shows photocatalytic properties at low wavelengths [21]. A refractive index of 2.43 causes a decrease in light transmittance in PV panels. Therefore, TiO_2 is used in combination with less index material, such as SiO_2. This combination allows us to increase the light transmittance while also reducing the reflection. As an alternative to TiO_2, studies use ZrO_2 and ZnO with an index of 2.15 and 2.10, respectively [22]–[24]. Of these, ZnO has a 3.2-eV bandgap and shows similar properties to TiO_2 [25]. As a result of the combined use, the methods used in antireflection coatings are also applied to the TiO_2. It has been observed that SiO_2 and TiO_2 are used with polyvinylpyrrolidone (PVP), polyacrylonitrile (PAN), polyurethane (PU), polyvinylalcohol (PVA), polyvinyl acetate (PVAc), and polymethylmethacrylate (PMMA) polymers as binding and holding together [13]. Due to the use of TiO_2, a hydrophobic surface, which is described as the water droplets being repelled from the surface to form a ball shape, is obtained [26]. A superhydrophobic surface was obtained in the literature by increasing the water contact angle (WCA) above 150° in self-cleaning studies [27]. Thus, a water droplet is repelled from the surface by reducing its contact with the surface, and the surface is cleaned by rolling. Some similar studies using electrospinning or sol-gel in the literature were examined below.

A coating using electrospinning and SiO_2 was applied one side and both side of PV. 1.2-g PVAc was used as a polymer. PVAc was mixed with 10-ml dimethyl acetamide, 2-ml acetic acid (CH_3COOH), and 1-ml tetraethoxysilane (TEOS). The transmittance of glass coated on one side was increased to 94.3% and the transmittance of glass coated on both sides was increased to 96% [28]. Nanofibrous PVP/SiO_2 composites were obtained by electrospinning and after calcination at a temperature of 600 °C. In this article, the PVP ratio was 10% in ethanol (CH_3CH_2OH), to which a mixture of CH_3COOH/TEOS precursors [29]. A porous or not SiO_2 ARC was applied on both sides of 24 glasses. To optimize the coating and to increase the transmittance was used as genetic algorithm. The relationship between coating thickness and SiO_2 porosity in different glasses was investigated [30]. The WCA of the polytetrafluoroethylene (PTFE)-SiO_2 coating prepared by the gel-gel and dip-coating method reached 97.02°, and the average transmittance was 97.86% [31]. TiO_2/SiO_2 hydrophobic single-layer thin film was obtained by spraying and dip-coating methods. It was measured that there is no difference in electrical power output between coated versus uncoated panels in two monthly outdoor tests. Overall panel efficiency decreased from 12.50% to 12.54%, so need to test long-term analysis [32].

This study aims to provide antireflective and self-cleaning properties with the coating made on the cover glass of PV panels. Depending on the increase in power output in the coated PV panel, an increase in efficiency is aimed. At the same time, by

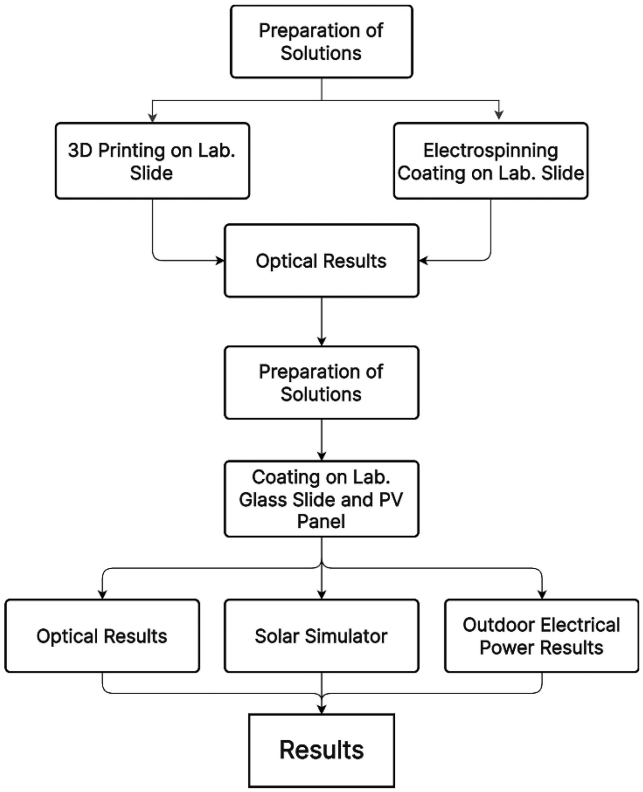

Fig. 3. Flowchart of experimental.

TABLE I
SOLUTION CONTENTS

Sol. No.	Polymer		$CHCl_3$ (ml)	SiO_2 (g)	TiO_2 (g)
	PLA (g)	PMMA (g)			
1	-	2	20	0.1	0.1
2	1.6	-	20	0.2	0.2
3	2	-	20	0.1	-
4	2	-	20	-	0.1
5	2	-	20	-	0.05
6	1.6	-	20	0.05	0.05
7	2	-	20	0.05	-
8	1.6	-	20	0.025	0.025
9	-	1.6	20	0.025	-
10	-	1.6	20	0.025	0.025
11		1.6	20	0.05	0.05
12	2	-	20	0.05	0.05

providing a hydrophobic property, it is aimed that coatings have antiwater, anti-icing, antifogging, and antidusting properties. Antireflective and self-cleaning coatings have been developed with sol + electrospinning and sol + 3-D printer as a new method. The solution and 3-D printer parameters required to apply antireflective and self-cleaning coatings with a 3-D printer were determined experimentally. With the technique used in the study, it is aimed that the coatings be applied quickly, cost-effective, practical, and portable.

II. MATERIAL, METHOD, AND EXPERIMENTAL DETAILS

The experimental study consists of four stages. Preparation of solutions, applying coatings, optical and electrical measurements, and real-time comparison in an outdoor environment. At the end of the study, coated PV panels with five different characterizations were obtained and tested outdoors. The processes of the experimental study can be seen in Fig. 3.

A. Materials

SiO_2 was purchased from Nanokar with amorphous, purity 99.5%, average particle size 10–20 nm, and nonporous. TiO_2 was purchased from Nanokar with rutile, purity 99.5%, average particle size 10–30 nm. Polylactic acid (PLA) biopolymer with a 3-mm nominal granule size, and PMMA with a weight average milliwatt of ∼15 000 and a powder were obtained from Marmara University Center for Nanotechnology and Biomaterials Applications and Research (NBUAM). Chloroform ($CHCl_3$) with a molecular weight of 119.37 (g/mol), CH_3COOH with a molecular weight of 60.05, and CH_3CH_2OH with a molecular weight of 46.07 were obtained from NBUAM Marmara University.

B. Preparation of Sol

Twelve solutions that have a different characterization were prepared by simplifying them according to concentration possibilities. Thus, the possibilities of all parameters have not been tested, and time and labor are saved. The details of the applied solutions can be seen in Table I. Base materials (SiO_2, TiO_2), binders(polymers), and solvents are similar in solutions. $CHCl_3$, CH_3COOH, and CH_3CH_2OH were used as solvents. $CHCl_3$ chosen as the solvent is known to be a suitable solvent for PLA [33]. CH_3COOH and CH_3CH_2OH have been tested to examine their effect on solution and printing methods. PLA, used as a binding polymer material, was chosen due to its 180 °C melting point, 90% light transmittance, and 1.482–1.492 refractive index properties [34], [35]. As an alternative to PLA, PMMA was used because it is close to PLA with a 160 °C melting temperature, 92% light transmittance, and 1.49 refractive index [36].

According to the optical measurement results among 12 solutions, formulations of the solution-68 and 12 were used as main formulas and prepared again for coating purposes. The solutions prepared same concentration were halved in quantity. The reprepared solutions were coated again on laboratory glass for data verification before coating on the cover glass.

The viscosity problem was encountered in sol-1 and sol-11, and the coating could not be applied. In sol-4, 2 g of PLA and 20 ml of $CHCl_3$ were mixed for 3 h, then TiO_2 was added and

stirred for another 2.5 h. Finally, 1.5-ml CH_3CH_2OH and 1.5-ml CH_3COOH were added to the mixture and stirred for another 1 h. So, the effect of CH_3CH_2OH and CH_3COOH on the solution was investigated.

While preparing solution-6 (sol-6), first, 20 ml of $CHCl_3$ and 1.6 g of PLA (8% polymer in solvent) were added to a beaker, and its volatility was prevented by covering with parafilm. Next, it was mixed in a magnetic stirrer (Daihan MSH-20A) at 1000 r/min for 2 h at 25 °C ambient temperature, wholly dissolved and homogenized. The particle sizes of TiO_2 and SiO_2 used as base materials are 28 and 22 nm, respectively. Finally, 0.05-g SiO_2 and 0.05-g TiO_2 were added simultaneously and stirred under the same conditions by preventing volatility for 3 h more.

Solution-12 (sol-12) was prepared by stirring 2 g of PLA and 20 ml of $CHCl_3$ (10% polymer in solvent) for 2 h under sol-6 preparation conditions. Then, 0.05-g SiO_2 and 0.05-g TiO_2 were added and stirred all for 2.5 h.

Solution-8 (sol-8) was mixed with 20-ml $CHCl_3$ and 1.6-g PLA (8% polymer-solvent ratio) for 2.5 h under the conditions of sol-6 and homogenized. At the end of 2.5 h, 0.025 g of SiO_2 and 0.025 g of TiO_2 were added and stirred for four more hours without changing the same conditions.

C. Methods

Two methods were used for coating the prepared solutions. These methods are the 3-D printer and electrospinning method. Since sol-1 and sol-11 were not used due to viscosity problems, the remaining ten solutions were used with different parameters of these methods.

1) 3-D Printer: Unlike using a 3-D printer with filament, Ultimaker 2+ (modified for bioprinting) with a kit that can work with a solution was used. First, the prepared solutions were coated with a single layer on a microscope slide (standard laboratory microscope glass, soda-lime glass, 25 × 75 mm, 1 mm thickness, precleaned). After optical measurements, Sol-6, Sol-12, and Sol-8 were printed on PV panels (83 × 66 mm, noncurved edge, 3.30-V V_{oc}, 68-mA I_{sc}). Solution and 3-D printer can be seen in Fig. 4. 3-D parameters are infill ratio, extruder multiplier, extruder width, primary layer height, *X*/*Y* axis movement speed, and printing speed. The fixed 3-D parameters of five different coatings made on PV panels; Extruder multiplier: 1.5, extruder width: 0.20 μm, primary layer height: 0.05 mm, *X*/*Y* axis movement speed: 4800 mm/s, and printing speed: 300 mm/s. Extruder multiplier (Ext. Mp.) is the printing speed, and therefore it means the flow rate of the solution from the injector needle.

The flow rate depends on the viscosity of the solution. Extruder multiplier (ml/min) was experimentally tested one by one by keeping other parameters fixed for three solutions, and it was decided to be 1.5. Since it is a 2-D design, the infill ratio was the variable parameter, whereas the other parameters were kept fixed in all coatings. The infill ratio is about how much space the needle's path when printing the following line. So, this means the distance between the lines. To examine the effect of the infill ratio and to reveal the correct infill ratio, different infill parameters were tried in the same solution type. Since the extruder width is 0.20 μm, it has been experimentally found that the infill ratio value should not exceed 50% to prevent the lines from overlapping. This value is related to the viscosity of the solution. It is observed that different infill ratio values have been shown to affect the formation of spaces or uniform patterns between lines.

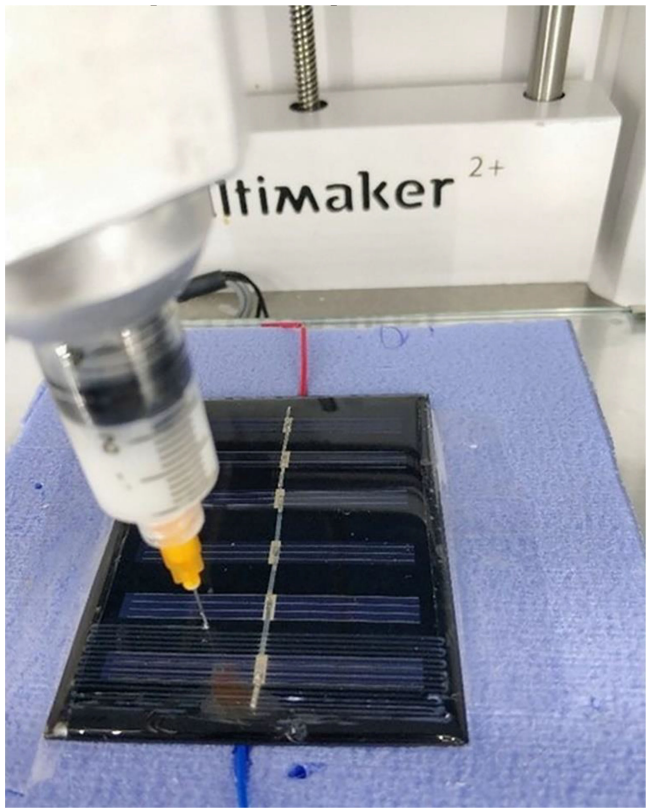

Fig. 4. 3-D printer application.

TABLE II
3-D PARAMETERS

Sol	Sample and PV	Infill Ratio (%)
6	1	35
6	2	20
12	3	40
8	4	50
8	5	35

First, the coating was made on the slide to obtain the data verification and optical results of the coating made with a 3-D printer. Then, the coating had been applied to the PV panel without changing any parameters. As a result of the process, it was seen that 3 ml of the prepared solution was used for each panel surface area. Infill ratio values that vary in PV panel coating are given in Table II.

TABLE III
PARAMETERS OF ELECTROSPINNING

Flow Rate (ml/h)	Voltage (kV)	Time (sec)	Distance (cm)
0.1	16	60	10
0.2	20	120	15
0.3	22	150	
0.5	24	180	
		210	
		240	
		300	

2) Electrospinning: Electrospinning is a known method used for antireflective and self-cleaning coatings. Electrospinning parameters are flow rate (ml/h), voltage (kV), application time (s), and distance (cm). Application values of electrospinning method parameters can be seen in Table III.

In the electrospinning method, different contents were applied with varying combinations of the parameters in Table III, but the desired results were not achieved. In coatings, nonadhesion to the surface, no homogeneous pattern, and high coating thickness were observed, and the highest 66% value was obtained in optical results. For this reason, only the 3-D printer was used in the second phase of the study.

D. Characterization

Slide glass surfaces coated with a 3-D printer were examined under an optical microscope (Olympus–Colorview). The focused criteria on the microscope are line formation, surface adhesion, line breakage, pattern and line homogeneity, dispersion of SiO_2 and TiO_2 materials on the surface, and their response to light. In addition, fiber formation, nanoparticle transfer, connection to each other fibers, and pattern of coatings made by electrospinning were investigated. 5x-10x-20x images were taken with the optical microscope.

The ratio of light transmission between the receiving and transmitting beam source is called Transmittance% (T%). After optical imaging, light transmittance (T%) was measured at room temperature with UV-VIS spectrophotometer (PG Instrument-T60). UV-Visible spectrophotometer measurements were made with the following steps, respectively, measurement of base laboratory glass, calibration, and measurement of samples. In the measurement, samples were placed close to the light beam source. The spectrum of wavelength was set between 300–800 nm.

The samples of the coatings on the sliding glass were vacuumed for scanning electron microscopy (SEM) analysis with the sputter coater (Quorum SC7020) and then gold–palladium coated by giving argon gas for 120 s under 15-mA current. After sputter coater, coating thickness measurement and energy dispersive X-ray spectroscopy (EDS or EDX) analysis were performed with the SEM (Zeiss EVO MA-10).

TABLE IV
LIGHT TRANSMITTANCES OF COATINGS

Sol. No.	Electrospinning		3D Printer	
	T% at 550 nm	T% Peak	T% at 550 nm	T% Peak
2	52	52.6	52.1	52.9
3	27.1	27.9	86.8	86.9
4	60.9	61.7	63.4	70.5
5	18.5	20.7	75.2	78.3
6	54.5	59.5	84.3	84.8
7	66.2	66.3	88.2	88.4
8	64.8	65.4	82.2	84
9	40.4	54.8	80.7	82.3
10	51.7	53.2	16.7	17.9
12	64.4	64.5	81.9	83

WCA measurements were performed with a PGX+ goniometer. Coated laboratory glass slides as samples were analyzed. The embedding needle method was used for the measurement of contact angle. A 1 μl of a distilled and deionized water droplet was injected at a speed of 0.2 μl/min and the droplet touches the sample surface. Then, while the needle tip was inside, the droplet was injected at a speed of 0.2 μl/min and a volume of 5 μl. And then, the volume of the 5-μl drop was increased to 25 μl with a speed of 0.2 μl/min without retracting the needle, and the volume of the water dropping was reduced to 5 μl with a speed of 0.2 μl/min while the needle pulling back.

After realizing the coating on the PV panel, *I–V* curve graphs were obtained with the solar simulator (Luzchem-SolSim, AM1.5, 1000 W/m^2) under the simulator test standard condition before the outdoor electrical measurements. An uncoated panel and five coated panels were tested, and the simulator results are given in Fig. 9.

III. RESULTS

A. Optical Results

The same laboratory slide glass was used for the measurements of both coatings and the blank light transmittance measurement was 91.7%. The light transmittances of the coatings made with ten different solutions are given in Fig. 5 and Table IV. Table IV was created according to the data in Fig. 5. The light transmittance of the sol-2 coating was measured to be the same T% in both methods. The light transmittance of the 3-D printer coatings is higher than the coatings made with electrospinning, except for the coating made with sol-2 and sol-10. According to

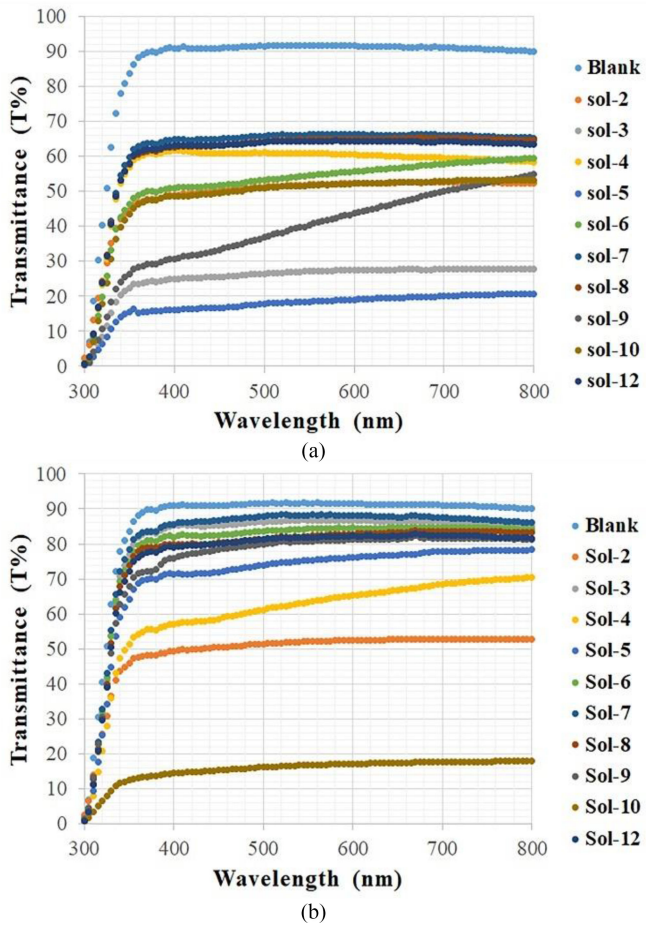

Fig. 5. %Transmittance of coatings. (a) Electrospinning. (b) 3-D printer.

the light transmittance measurements, it was seen that the 3-D printer method is more successful.

The peak light transmittances of the coatings of electrospinning were measured between 20.7%–66.3% [see Fig. 5(a) and Table IV]. In sol-3 and sol-5 coatings, which have the lowest light transmittance, the light transmittance was measured as 27.8% and 20.7% at the peak, but 27.1% and 18.5% at 550 nm, respectively. The sol-9 coating has shown variability in light transmittance at different wavelengths. The light transmittance of the coatings made with sol-9 was measured as 40.4% at 550-nm wavelength and 54.8% at the peak. Among other solutions, the highest light transmittance at 550 nm was measured as 66.2% in sol-7, given in Table IV. But in solutions containing SiO_2 and TiO_2, the peak value of light transmittance at 550 nm was observed at 64.8% in sol-8 and 64.4% in sol-12. In addition, in the analysis with the optical microscope, it was observed that the coating did not disperse homogeneously on the surface.

Fig. 5(b) shows that the peak of light transmittance of coatings made via a 3-D printer was measured between 52.9%–88.4%, excluding one mixture. Sol-10 coating was found to be an unsuccessful coating with a light transmittance of 17.9%. Sol-3, sol-6, sol-7, sol-8, sol-9, and sol-12 had more than 80% light transmittance. Although sol-3 and sol-7 coatings have the highest light transmittance, they were prepared with only SiO_2.

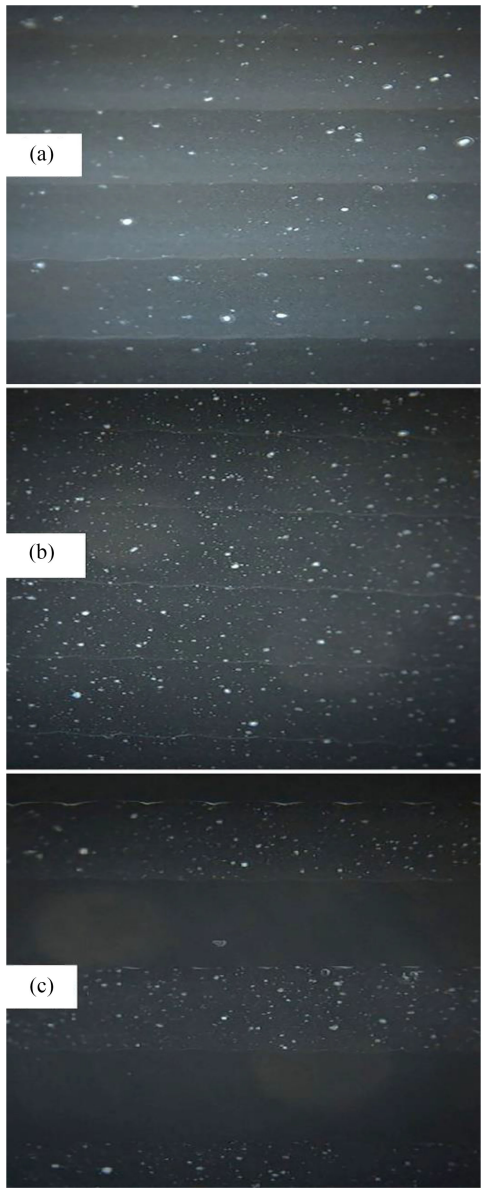

Fig. 6. Infill ratio effect on the line printing (a) %100, (b) %50, and (c) %20.

Sol-6, sol-8, and sol-12, which the best results were measured at 550 nm with 84.3%, 82.2%, and 81.9%, were selected for PV panel coatings. In optical microscope analysis of coatings, it was observed that the infill ratio between 35–50 provides an ideal line formation that is good forming and has no gaps. In the single-layer coating made with a 3-D printer, SiO_2 and TiO_2 nanoparticles are homogeneously spread on the surface. In Fig. 6, if the infill ratio parameter is high, overlapping lines can be seen, and if it is low, the gap between the lines can be seen.

Fig. 6(a) shows that the infill ratio is 100%, and transmittance decreases considerably due to overlapping lines. The ideal line formation was observed in the range of 35%–50% infill ratio according to the concentration ratio of the solution, as seen in Fig. 6(b). As in Fig. 6(c), when the infill ratio is 30% below, gaps between the lines and homogeneous coating cannot be obtained. In Fig. 6, SiO_2 and TiO_2 nanoparticles adhered to the surface

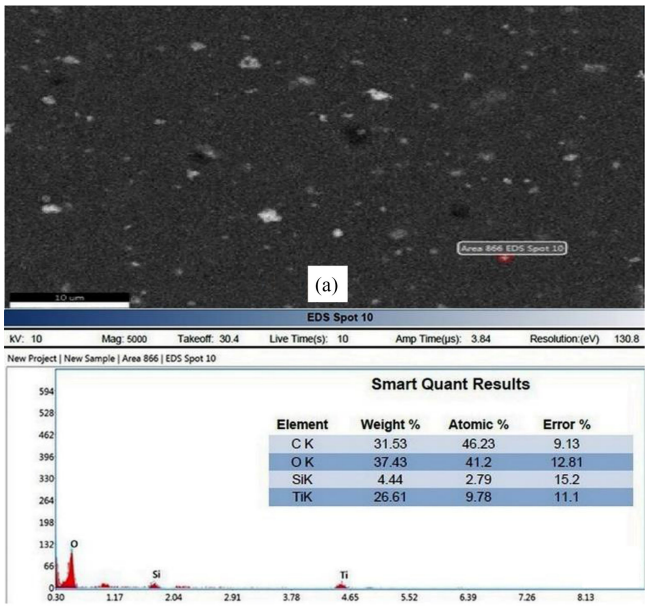

Fig. 7. (a) SiO_2 and TiO_2 nanoparticles. (b) EDS analysis.

and dispersed homogeneously can be seen in optical microscope analysis. In Fig. 7(a), the silicon and titanium nanoparticles that are spread on the surface, and in Fig. 7(b), the EDS (EDX) analysis result of the coating under the SEM can be seen. In the coatings, it was seen that no other elements were seen on the surface except SiO_2 or TiO_2 nanoparticles and only SiO_2 and TiO_2 nanoparticles were found on the surface. According to the EDS analysis that can be seen in Fig.7(b), it was found to be 4.44% wt. SiO_2 and 26.61% wt. TiO_2. The brightly colored nanoparticle seen in Fig.7(a) is TiO_2, and the dark-colored nanoparticle is SiO_2 nanoparticle.

The minimum thickness of the 3-D printer is 50 μm, so the coatings are made in this setting. The SEM analysis observed that the coating thicknesses are between 3.122–8.477 μm with evaporation at room temperature after coating (see Fig. 8).

B. Electrical Results

1) Solar Simulator: I–V graphics of each panel were obtained from the solar simulator test. Comparative *I–V* curves of the coated panels are given in Fig. 9.

According to the solar simulator test result, the peak power output of the uncoated panel was calculated as 218 mW. The coated PVs' peak power outputs are as follows. PV-1178 mW, PV-2215 mW, PV-3218 mW, PV-4221 mW, and PV-5223 mW. According to these results, it was measured that the uncoated PV generates more power than PV-1 and PV-2 and has a power output equal to PV-3. It was measured that PV-4 and PV-5 panels give more power output than the uncoated panel. An outdoor performance test was performed to analyze the solar simulator results in real time.

2) Outdoor Electrical Power Performance: For the outdoor test of the coated panels, two multimeters (UNI-T UT803, desk type) with calibration certificate of the same date were measured

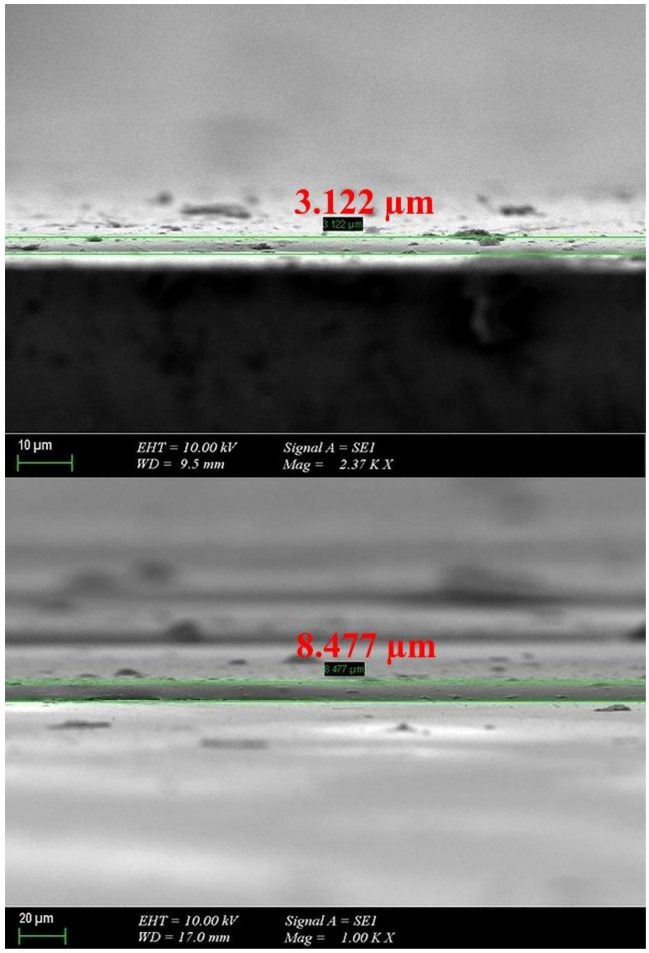

Fig. 8. Coating thickness.

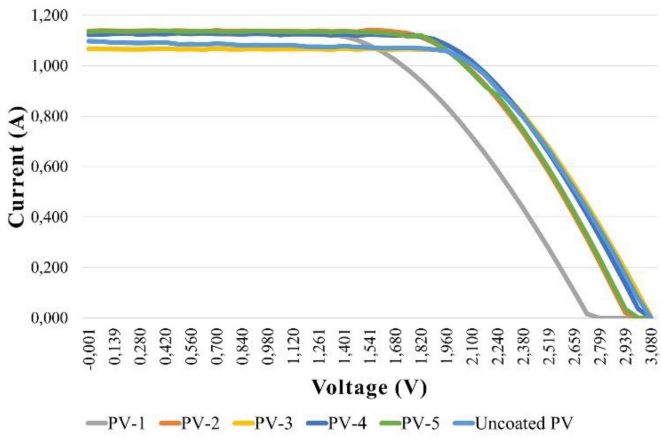

Fig. 9. *I–V* curves.

for ten days at intervals of 30 s, and 28 800 data were obtained for each ten-day measurement. The experimental setup was prepared for the outdoor test at the coordinates 37.04N-35.30E and shown in Fig. 10. In the experimental circuit, the *R*th value calculated from V_{oc} and I_{sc} was 53 Ω for the maximum power of PV panels. The load power (Pr) was calculated with the formula $P = Vr^2/R$ from the voltage (Vr) falling on the R resistor.

Fig. 10. Electrical experimental setup.

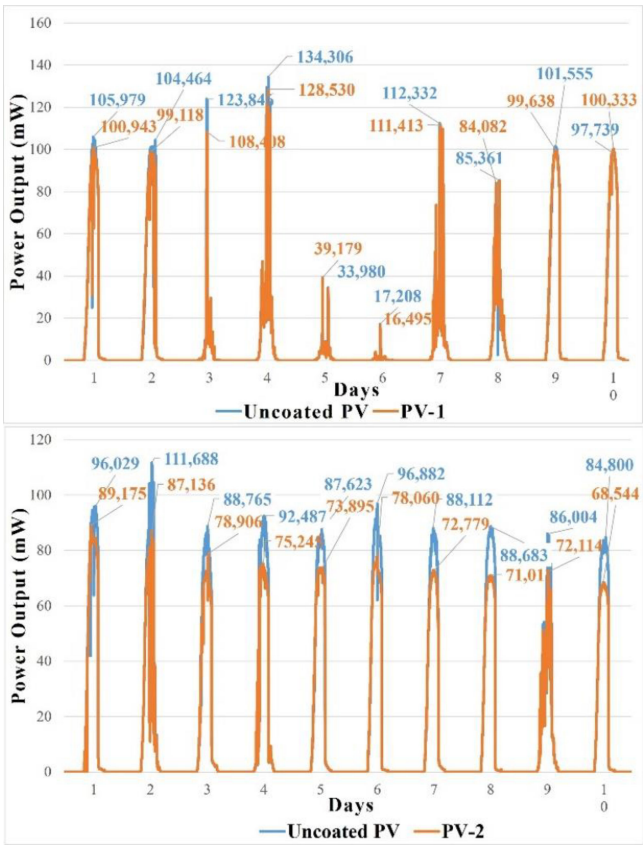

Fig. 11. Solution-6 (PV-1, PV-2) daily power output.

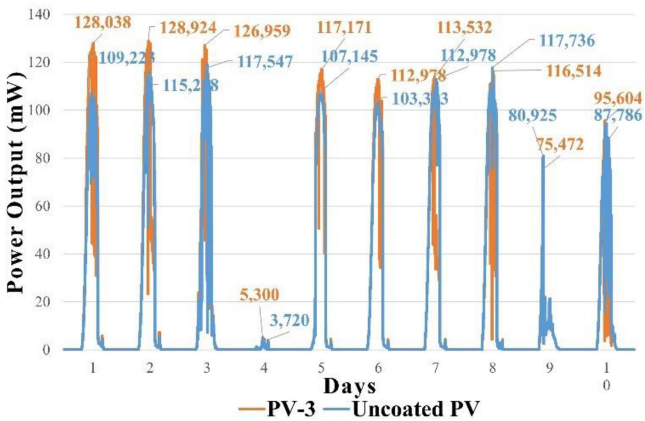

Fig. 12. Solution-12 (PV-3) daily power output.

Both panels are connected in series with the same type of 53-Ω resistor. The panels are positioned south (azimuth 180°) and parallel to the ground (tilt 0°). At the same time, the panels are positioned so that they are not shaded from sunrise to sunset and by providing isolation.

The panels were measured as coated–uncoated in ten-day periods. The comparisons of experimental measurements repeated five times with different coated panels are given in Figs. 11–13. In the figures, the panels prepared with the same solution are presented together. Power output is the load power (Pr) in Figs. 11–13. Power outputs data are logged under different weather conditions classified as cloudy–partly cloudy–clear.

The daily energy production (mWh/day) of the panels was obtained by multiplying and adding the instantaneous power data obtained in the measurements made under outdoor conditions by the measurement intervals. Then, the power output was converted into energy production. Finally, the energies produced were compared, and the PV-5 with the best result is shown in Fig. 14.

After the daily total energy production was given, the ten-day total energy production of all coated and uncoated panels was calculated. Thus, all figures were converted to the same data type shown in Table V, and the difference was compared for ten days.

Weather conditions must be evaluated to interpret the power curves. The ten-day total energy outputs of all panels were compared, and the gains for ten days were calculated. Daily solar radiations (kWh/m^2) and daily sunshine durations (h) data obtained from the Turkish State Meteorological Service for the

TABLE V
PV'S TEN DAYS TOTAL ENERGY OUTPUTS AND GAINS

PVs	Coated-PV (mWh)	Uncoated-PV (mWh)	Gain (%)
PV-1	2187.749	2185.347	+0.11
PV-2	3062.794	3436.501	-10.875
PV-3	3127.979	3700.825	-15.479
PV-4	3350.749	3204.686	+4.558
PV-5	4922.398	4511.246	+9.114

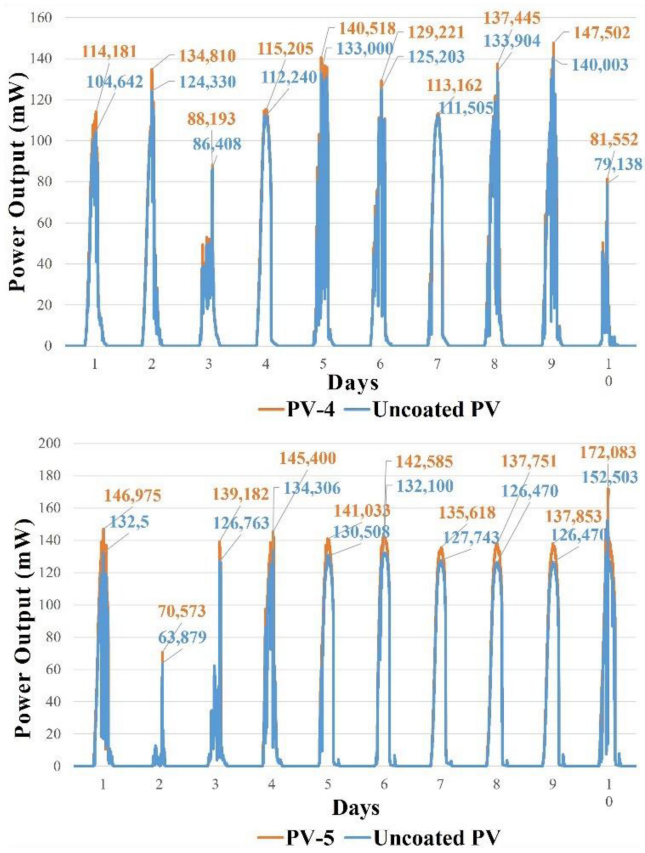

Fig. 13. Solution-8 (PV-4, PV-5) daily power output.

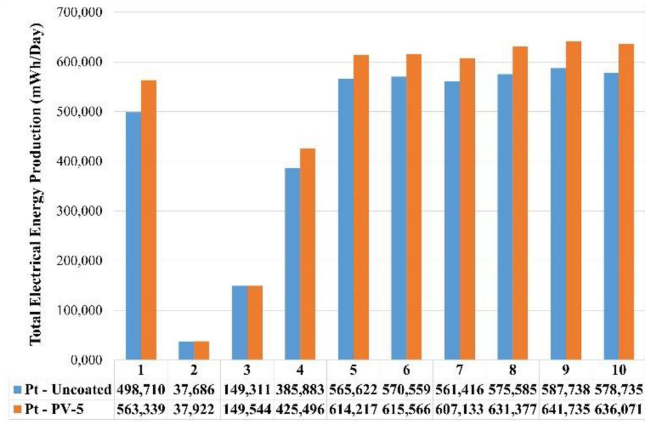

Fig. 14. Daily total energy production of PV-5.

exact coordinates are proportioned according to the surface area of the panels.

The daily recorded weather conditions, which are classified as Clear(*) – Partially Cloudy(**), and Cloudy(***), and the daily sunshine duration (h) are given in Table VI. Clear days are unclouded and sunny days, partial cloudy is half sunny–half cloudy days, and cloudy is dark, sunless, or rainy days.

Daily sunshine duration is added to these figures. In this way, an influential figure was provided by establishing a relationship with the weather in Table VI. Finally, the daily efficiencies of the panels were calculated by proportioning the electrical energy

TABLE VI
WEATHER CONDITION AND SUNSHINE DURATION (H) ON TESTING DAYS

Days	PV-1	PV-2	PV-3	PV-4	PV-5
Day-1	* / 8	* / 8.0	* / 8.4	** / 5.7	** / 7.4
Day-2	*/ 7.8	** / 6.8	** / 8.4	** / 6.4	*** / 0.3
Day-3	***/ 0.6	* / 7.9	** / 6.6	*** / 3.9	*** / 1.4
Day-4	** / 5.7	* / 6.4	*** / 0.0	* / 8.1	** / 5.2
Day-5	*** / 0.0	* / 7.9	* / 6.4	*** / 6.7	* / 7.7
Day-6	*** / 0.0	* / 7.9	* / 8.2	*** / 7.7	* / 7.6
Day-7	** / 2.7	* / 7.9	** / 8.2	* / 7.8	* / 8.2
Day-8	*** / 1.7	* / 7.9	** / 8.0	** / 5.3	* / 8.3
Day-9	* / 8.0	** / 6.2	*** / 1.6	** / 6.4	* / 8.4
Day-10	* / 8.0	* / 8.0	** / 6.0	*** / 0.7	** / 8.2

Note: Clear (*), partial cloudy (**), and cloudy(***).

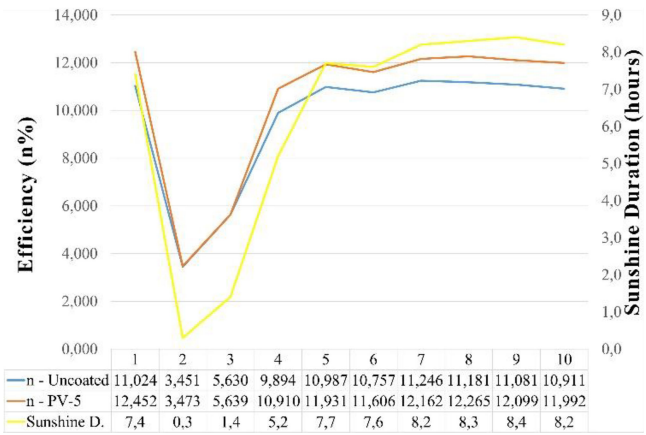

Fig. 15. Daily efficiency of PV-5.

produced in return for the daily solar radiation in a square meter to the cell size, and the PV-5 with the best performance is given in Fig. 15.

After the ten-day efficiency and sunshine duration data of five PV panels are given, the ten-day average efficiency differences as a percentage are shown in Table VII.

IV. DISCUSSION

If a comparison is made according to solution contents, in terms of light transmittance (T%), surface adhesion, viscosity, and homogeneity, Sol-6, Sol-12, and Sol-8 mixtures are 1.6 – 2 – 1.6 g PLA polymer, SiO_2 and TiO_2 were both 0.05-0.05- 0.025 g, respectively. Although PMMA polymer is used in the same and different ratios, satisfactory results have not been achieved. The problems in PMMA polymer are inadequate surface adhesion, viscosity, and low light transmittance. The highest light transmittance in PMMA coatings is sol-9, which

TABLE VII
PV'S TEN DAYS AVERAGE EFFICIENCY AND GAINS

PVs	Coated-PV (n%)	Uncoated-PV (n%)	Gain (%)
PV-1	6.482	6.480	0.027
PV-2	7.645	8.565	-10.735
PV-3	7.316	8.634	-15.269
PV-4	9.487	9.066	4.654
PV-5	10.453	9.616	8.700

has containing only SiO_2 80.7% at 550 nm (82.3% at peak) applied by the 3-D printer.

The light transmittances of sol-6, sol-12, and sol-8 seen in Fig. 5(b) were measured as 84.3%, 81.9%, and 82.2% specifically at 550 nm, respectively. The light transmittances of verification coatings in the second stage of the study were measured as sol-684.8%, sol-12 84%, and sol-883%. It has been observed that the light transmittances are approximately the same in coatings made with a 3-D printer using the same parameter and solution contents.

In solution preparation, the polymer was dissolved, and then nanoparticles were added. The solution and the addition intervals of SiO_2 and TiO_2 nanoparticles from 1 to 24 h were found experimentally. Thus, it has been seen that it is ideal for dissolving the polymer by mixing for 2–2.5 h, and then adding the nanoparticles and stirring for another 2.5–4 h are sufficient but stirring in close to 4 h is appropriate in terms of homogeneity.

It has been observed that the electrospinning voltage in the range of 16–24 kV and the flow rate in the range of 0.1–0.5 ml/h are appropriate. However, a homogeneous coating on the surface area could not be obtained in this method. The problems encountered are frequently nozzle clogging, surface adhesion, very low light transmittance, and accumulation of the coating around the center point of the surface, which leads to an increase in coating thickness around a circle. Different combinations of distance–voltage–flow rates have been tried but have not successfully prevented accumulation around a point. In future studies, it is aimed to focus on this problem.

The application with the 3-D printer is easy, practical, and no additional processing is required after the process. It has been seen that cover glass coatings of panels in current commercial use can be made by mobilizing this method. Moreover, there is no parameter change requirement for panels of the same size and specification. In these aspects, the 3-D printer coating method provides an advantage. Extruder multiplier (Ext. Mp.) was found experimentally for each solution depending on the viscosity. After printing the first line, attention was paid to ensure that the solution dried on the surface until the next line. When the solution has not dried if Ext. Mp. is high, the lines merge with next and previous and a homogeneous line, so the coating is not formed. If Ext. Mp. is low, line formation is not fully developed due to the low solution flow rate, and breaks are observed in the line. Ext. Mp. had been optimized as 1.5 ml/min and applied.

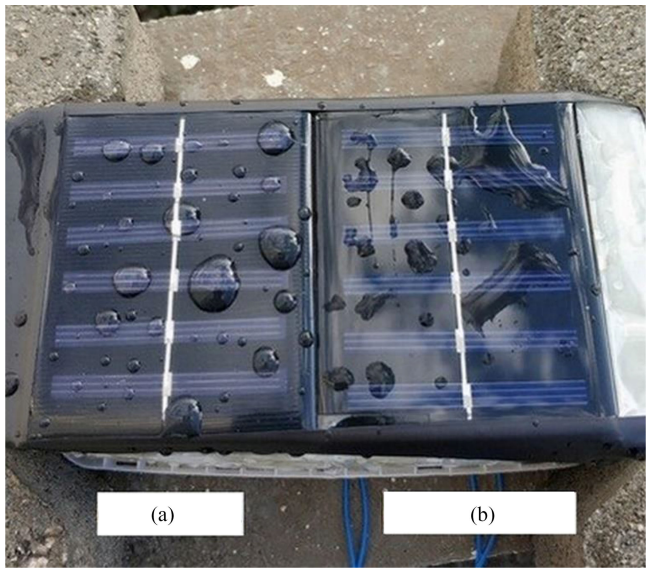

Fig. 16. Hydrophobic effect on coated PV versus uncoated PV. (a) Coated. (b) Uncoated.

Different results were examined by adjusting the infill ratio (or percentage). It was observed that the infill ratio value should be in the range of 35–50 (see Fig. 6). Although only the PV-3 panel was prepared with solution-12, the surface adhesion and line spacing were good. The infill ratio of 40 used failed to generate more electrical energy since it was denser than other solutions with 2-g PLA and 0.05-g SiO_2 and TiO_2.

When SEM examined the coating thicknesses and EDS analysis, it was seen that the 50-μm coating thicknesses decreased between 3.12–8.47 μm with the volatility of the solvent after the minimum thickness coating, which is the sensitivity of 50 μm. It is planned to research the coating thicknesses and light transmittance to be made with a more sensitive 3-D printer in future studies. When thinner coating thickness is applied, it is expected to decrease to nanometer thickness with the effect of volatility. In the EDS analysis, it was observed that the SiO_2 and TiO_2 nanoparticles in the solution were spread evenly on the surface, and there were no other elements on the surface [see Fig. 7(b)].

With the use of SiO_2 and TiO_2 nanoparticles, in addition to the antireflective aimed in the study, self-cleaning was obtained, as seen in Fig. 16. In the image taken after the rain, it was observed that a hydrophobic surface was formed. While water drops spread on the surface of the uncoated panel, it is seen that the water drops gather together on the coated panels.

The hydrophobic surface seen in Fig. 16 was analyzed as mentioned in Section II-D. The WCA was measured as 96.18°, as seen in Fig. 17. Surfaces with a contact angle of more than 90° are defined as hydrophobic, and surfaces with a contact angle of more than 150° are considered superhydrophobic. Surfaces with a contact angle of less than 90° are defined as hydrophilic. The contact angle of the uncoated PV panel surfaces is unknown. However, it is observed that the hydrophobic surface is formed after the coating as seen in the contact angle on the surface. With the hydrophobic property obtained, the water droplets coming

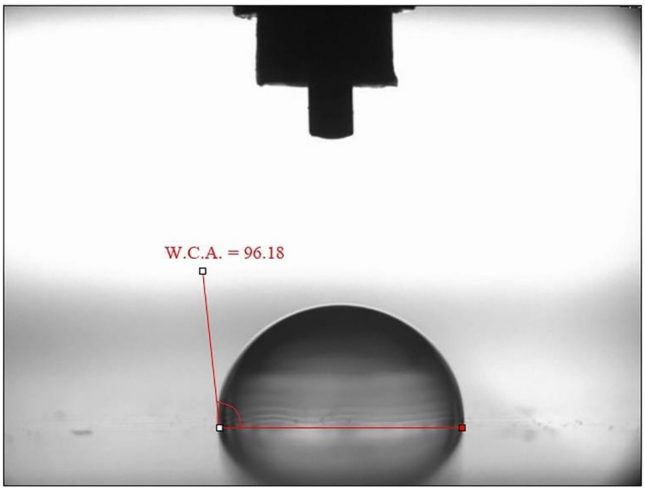

Fig. 17. WCA measurement.

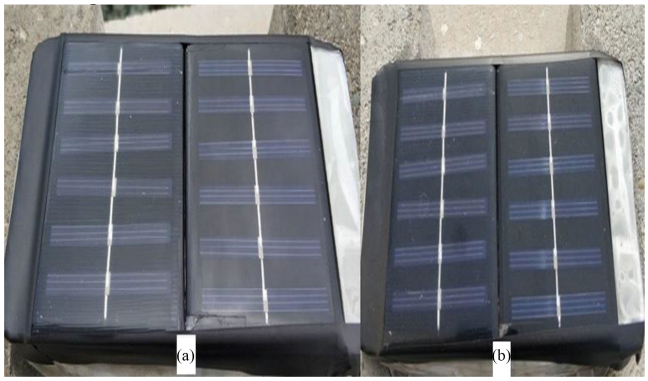

Fig. 18. (a) Beginning of testing. (b) Ending of testing.

to the surface collect dirt, dust, and organic waste and flow from the surface. In this way, the self-cleaning feature is provided. In a similar AR coating made with the SiO_2 sol-gel method, the light transmittance decreased by 7.56%, whereas the WCA was increased from 22% to 130% [37]. In another study, it was observed that the light transmittance decreased from 89% to 85% in a coating obtained by using a 7% SiO_2-TiO_2 ratio and a spin-coating technique using a polycarbonate [38]. A coating containing 1.5 wt% SiO_2-TiO_2 was fabricated with a hydrophilic and superior self-cleaning performance and light transmittance was measured as 89.57% [39]. Although the methods used in similar studies in the literature are different, the coatings are comparable in terms of nanoparticle, WCA, hydrophobicity, self-cleaning, and light transmittance.

Cloudy days are, not all, but mostly rainy days. After these days, more power output was obtained on all PV panels. It has been evaluated that cleaning the surface with hydrophobic properties contributes to obtaining more power output on PV-4 and PV-5 panels.

As shown in Fig. 18, there is less dust accumulation on the coated panel at the end of the test duration. This study can be developed to offer anti-icing, antifogging, and antidusting properties by achieving a superhydrophobic surface [40]. In future studies, it has been seen that it should be tested for a long-time duration and in different climatic conditions with the tilted setup.

The daily power output was obtained from the ten-day outdoor performance test of all coated and uncoated panels separately, and Table V was derived from them by transforming. In PV-1, it was observed that a hydrophobic surface was formed on the surface of the panel for ten days, and the pollution was reduced on the panel surface. It was evaluated that the 3-D parameters were selected correctly in the PV-1 panel, but there were deficiencies in terms of solution content despite the hydrophobic surface. In PV-2, which is a failed coating, it was thought that the infill ratio of 20 creates a gap between the lines, which leads to a decrease in efficiency and power output. In the PV-3 panel, the main reason for failure can be seen that sol-12 contains 2 g of polymer and 25% more polymer than the others. Another reason can be seen as the infill ratio applied as 40 in the sol-12. In the PV-4, the total energy production for ten days increased by 4.558%, and the ten-day average efficiency was 4.654% more.

The PV-5 panel is similar to the PV-4 in all weather conditions, and it produces more energy and more panel efficiency than the uncoated panel. On the second and third days seen in Fig. 15, there were 0.3 and 1.4 h of sunshine duration due to the cloudy weather, and the least efficiency difference was realized 0.625% and 0.156% on these days. The highest efficiency increase was achieved on the first and fourth days when the weather is partly cloudy. The PV-5 panel reached 12.959% and 10.266% more efficiency in these two days than the uncoated. On other days when the weather is clear, the efficiency increases are between 7.8%–9.9%, and the ten-day average efficiency gain is 8.7%. As with other surfaces, a hydrophobic surface was observed during the observation carried out in cloudy weather conditions corresponding to rainy days (see Fig. 16). The difference at the end of the test between PV-4 and PV-5, derived from sol-8, can be explained as the infill ratio effect.

V. Conclusion

SiO_2 and TiO_2 nanoparticles were selected by the literature in this study, which was carried out with the aim of antireflection and self-cleaning. 3-D printer and electrospinning methods were used with PLA polymer. Different parameters of the method and different mixing ratios were experimentally tested. It was found that the appropriate polymer ratio was 1.6 g in 20 ml of $CHCl_3$, and the ideal nanoparticle weight was 0.025 g. Light transmittance of 83%–84.8% was measured in coatings on the laboratory glass slide. In 3-D parameters, it was found that the infill ratio and the extruder M.p. should be in the range of 35–50 and 1.5 ml/min, respectively. The thickness of the coating, which is a homogeneous and single layer, is between 3.12–8.47 μm. Among the panels tested for ten days in different outdoor climatic conditions, PV-4 and PV-5 prepared with sol-8 produced 4.558% and 9.114% more electrical energy than the uncoated panel. As a result, efficiency increases of 4.65% and 8.7% were achieved in PV-4 and PV-5. The WCA was measured as 96.18° and the hydrophobic property was obtained. In future studies, a study of coating will be made to increase the value of T% above of bare glass, and to increase the hydrophobicity

by increasing the WCA. In addition, the durability period of the coating, its long-term performance under different climatic conditions, and whether it will be degraded in the same climatic conditions (season) should be examined in future studies.

ACKNOWLEDGMENT

This study is derived from the doctoral (Ph.D.) dissertation titled "Nano-Structured Efficiency-Enhancing Coatings on Photovoltaic Panels" ("Fotovoltaik Panellerde Verim Artırıcı Nano Yapılı Kaplamalar" in Turkish) conducted at Marmara University. The authors would like to thank Marmara University Center for Nanotechnology & Biomaterials Applications and Research (NBUAM) for technical support.

A patent application has been made to TurkPatent, the official patent institution of the Republic of Türkiye, by application no: 2021/014398.

REFERENCES

[1] E. L. Christensen, "Solar concentrated photovoltaic systems using spectral splitting," Ph.D. dissertation, Inst. Optics, Univ. Rochester, New York, NY, USA, 2012.

[2] R. Brendel, *Thin-Film Crystalline Silicon Solar Cells: Physics and Technology*. Hoboken, NJ, USA: Wiley, 2003, pp. 157–180.

[3] L. Fraas and L. Partain, *Solar Cells and Their Applications*, 2nd ed. Hoboken, NJ, USA: Wiley, 2010, pp. 116–117.

[4] B. L. Sopori and R. A. Pryor, "Design of antireflection coatings for textured silicon solar cells," *Sol. Cells*, vol. 8, no. 3, pp. 249–261,1983. [Online]. Available: https://doi.org/10.1016/0379-6787(83)90064-9

[5] A. Goetzberger, J. Knobloch, and B. Vob, *Crystalline Silicon Solar Cells*. Hoboken, NJ, USA: Wiley, 1998, p. 89.

[6] G. Moona, P. Kapruwan, R. Sharma, and V. N. Ojha, "Silicon wafer surface reflectance investigations by using different surface texturing parameters," *Proc. Nat. Acad. Sci., India Sect. A: Phys., Sci.*, vol. 88, pp. 617–623, 2017. [Online]. Available: https://doi.org/10.1007/s40010-017-0384-3

[7] A. McEvoy, T. Markvart, and L. Castaner, *Solar Cells Materials, Manufacture and Operation*, 2nd. ed. Hoboken, NJ, USA: Elsevier, 2013, pp. 69–113.

[8] W. Abeygunasekara, V. Karunaratne, and P. Hiralal, "Numerical modelling of zinc oxide nanowire anti reflective coatings," in *Proc. IEEE 10th Int. Conf. Ind. Inf. Syst.*, 2015, pp. 244–249.

[9] Ö. Kesmez *et al.*, "Preparation and characterization of multilayer anti-reflective coatings via sol-gel process," *Ceramics Int.*, vol. 44, pp. 3183–3188, 2018. [Online]. Available: https://doi.org/10.1016/j.ceramint.2017.11.088

[10] W. Glaubitt and P. Löbmann, "Anti-reflective coatings prepared by sol-gel processing: Principles and applications," *J. Eur. Ceram. Soc.*, vol. 32, no. 11, pp. 2995–2999, Aug. 2012. [Online]. Available: https://doi.org/10.1016/j.jeurceramsoc.2012.02.032

[11] J. Zhi and L. Z. Zhang, "Durable superhydrophobic surface with highly anti-reflective and self-cleaning properties for the glass cover of solar cells," *Appl. Surf. Sci.*, vol. 454, pp. 239–248, Oct. 2018. [Online]. Available: https://doi.org/10.1016/j.apsusc.2018.05.139

[12] C. Agustín-Sáenz *et al.*, "Mechanical properties and field performance of hydrophobic anti-reflective sol-gel coatings on the cover glass of photovoltaic modules," *Sol. Energy Mater. Sol. Cells*, vol. 216, Oct. 2020, Art. no. 110694. [Online]. Available: https://doi.org/10.1016/j.solmat.2020.110694

[13] M. Ye *et al.*, "Design, fabrication, and modification of cost-effective nanostructured TiO_2 for solar energy applications," in *Low-Cost Nanomaterials Toward Greener and More Efficient Energy Applications*, Z. Lin and J. Wang, Eds. London, U.K.: Springer, 2014, pp. 15–44.

[14] K. Ali, S. A. Khan, and M. Z. M. Jafri, "Effect of double layer (SiO_2/TiO_2) anti-reflective coating on silicon solar cells," *Int. J. Electron. Chem. Sci.*, vol. 9, pp. 7865–7874, 2014. [Online]. Available: http://www.electrochemsci.org/papers/vol9/91207865.pdf

[15] A. Bake *et al.*, "Preparation of transparent and robust superhydrophobic surfaces for self-cleaning applications," *Prog. Org. Coatings*, vol. 122, pp. 170–179, Sep. 2018. [Online]. Available: https://doi.org/10.1016/j.porgcoat.2018.05.018

[16] C. Song and X. Dong, "Preparation and characterization of tetracomponent ZnO/SiO_2/SnO_2/TiO_2 composite nanofibers by electrospinning," *Adv. Chem. Eng. Sci.*, vol. 2, no. 1, pp. 108–112, Jan. 2012. [Online]. Available: http://dx.doi.org/10.4236/aces.2012.21012

[17] Q. Mao, D. Zeng, K. Xu, and C. Xie, "Fabrication of porous TiO_2-SiO_2 Multifunctional anti-reflection coatings by sol-gel spin coating method," *Roy. Chem. Soc. Adv.*, vol. 4, pp. 58101–58107, Oct. 2014. [Online]. Available: https://doi.org/10.1039/C4RA10424B

[18] M. M. Ahmad and A. Eshaghi, "Fabrication of anti-reflective superhydrophobic thin film based on the TMMS with self-cleaning and anti-icing properties," *Prog. Org. Coatings*, vol. 122, pp. 199–206, Sep. 2018. [Online]. Available: https://doi.org/10.1016/j.porgcoat.2018.06.001

[19] M. Zhong, Y. Zhang, X. Li, and X. Wu, "Facile fabrication of durable superhydrophobic silica/epoxy resin coatings with compatible transparency and stability," *Surf. Coatings Technol.*, vol. 347, pp. 191–198, Aug. 2018. [Online]. Available: https://doi.org/10.1016/j.surfcoat.2018.04.063

[20] S. B. Khan, H. Wu, C. Pan, and Z. Zhang, "A mini review: Anti-reflective coatings processing techniques, applications and future perspective," *Res. Rev.: J. Mater. Sci.*, vol. 5, no. 4, pp. 36–54, Oct. 2017. [Online]. Available: https://doi.org/10.4172/2321-6212.1000192

[21] A. Fouzia and B. Rabah, "The influence of doping lead and annealing temperature on grown of nanostructures of TiO_2 thin films prepared by a sol-gel method," *Mater. Sci. Eng.: B*, vol. 265, Mar. 2021, Art. no. 114982. [Online]. Available: https://doi.org/10.1016/j.mseb.2020.114982

[22] A. M. Law, L. D. Wright, A. Smith, P. J. M. Isherwood, and J. M. Walls, "2.3% efficiency gains for silicon solar modules using a durable broadband anti-reflection coating," in *Proc. 47th IEEE Photovolt. Specialists Conf.*, Calgary, AB, Canada, 2020, pp. 0973–0975.

[23] B. K. Ghosh, K. T. T. Kin, and S. S. M. Zainal, "Different materials coating effect on responsivity of Si UV photo detector," in *Proc. IEEE Conf. Clean Energy Technol.*, Langkawi, Malaysia, 2013, pp. 446–449.

[24] M. A. Eghfeli, S. A. Hadi, N. E. Atab, and A. Nayfeh, "Demonstration of aluminum doped ZnO as anti-reflection coating," in *Proc. IEEE 43rd Photovolt. Specialists Conf.*, Portland, OR, USA, 2016, pp. 2765–2769.

[25] A. Hagfeldt and M. Gratzel, "Light-induced redox reactions in nanocrystalline systems," *Chem. Rev.*, vol. 95, no. 1, pp. 49–68, 1995. [Online]. Available: https://doi.org/10.1021/cr00033a003

[26] I. Nayshevsky, Q. Xu, and A. M. Lyons, "Hydrophobic–hydrophilic surfaces exhibiting dropwise condensation for anti-soiling applications," *IEEE J. Photovolt.*, vol. 9, no. 1, pp. 302–307, Jan. 2019. [Online]. Available: https://doi.org/10.1109/JPHOTOV.2018.2882636

[27] S. Martin and B. Bhushan, "Transparent, wear-resistant, superhydrophobic and superoleophobic poly(dimethylsiloxane) (PDMS) surfaces," *J. Colloid Interface Sci.*, vol. 488, pp. 118–126, Feb. 2017. [Online]. Available: https://doi.org/10.1016/j.jcis.2016.10.094

[28] H. M. Raut *et al.*, "Porous SiO_2 anti-reflective coatings on large-area substrates by electrospinning and their application to solar modules," *Sol. Energy Mater. Sol. Cells*, vol. 111, pp. 9–15, Apr. 2013. [Online]. Available: https://doi.org/10.1016/j.solmat.2012.12.023

[29] W. Matysiak and T. Tanski, "Analysis of the morphology, structure and optical properties of 1D SiO_2 nanostructures obtained with sol-gel and electrospinning methods," *Appl. Surf. Sci.*, vol. 489, pp. 34–43, Sep. 2019. [Online]. Available: https://doi.org/10.1016/j.apsusc.2019.05.090

[30] A. Grosjean, A. Soum-Glaude, P. Neveu, and L. Thomas, "Comprehensive simulation and optimization of porous SiO_2 antireflective coating to improve glass solar transmittance for solar energy applications," *Sol. Energy Mater. Sol. Cells*, vol. 182, pp. 166–177, Aug. 2018. [Online]. Available: https://doi.org/10.1016/j.solmat.2018.03.040

[31] X. Sun *et al.*, "Preparation of hydrophobic SiO_2/PTFE sol and antireflective coatings for solar glass cover," *Optik*, vol. 212, Jun. 2020, Art. no. 164704. [Online]. Available: https://doi.org/10.1016/j.ijleo.2020.164704

[32] A. Soklic, M. Tasbihi, M. Kete, and U. L. Stangar, "Deposition and possible influence of a self-cleaning thin TiO_2/SiO_2 film on a photovoltaic module efficiency," *Catalysis Today*, vol. 252, pp. 54–60, Sep. 2015. [Online]. Available: https://doi.org/10.1016/j.cattod.2014.10.021

[33] A. Södergard and M. Stolt, "Properties of lactic acid based polymers and their correlation with composition," *Prog. Polym. Sci.*, vol. 27, no. 6, pp. 1123–1163, Jul. 2002. [Online]. Available: https://doi.org/10.1016/S0079-6700(02)00012-6

[34] A. J. Muller, M. A´Vıla, G. Saenz, and J. Salazar, "Crystallization of PLA-based materials," in *Poly(Lactic Acid) Science and Technology Processing, Properties, Additives and Applications*. London, U.K.: Roy. Soc. Chem., 2014, pp. 66–98.

[35] C. M. B. Goncalves, J. A. P. Coutinho, and I. M. Marrucho, "Optical properties," in *Poly(Lactic Acid): Synthesis, Structures, Properties, Processing, and Applications*. Hoboken, NJ, USA: Wiley, 2010, pp. 97–112.

[36] V. Bernardo *et al.*, "Low-density PMMA/MAM nanocellular polymers using low MAM contents: Production and characterization," *Polymer*, vol. 163, pp. 115–124, Feb. 2019. [Online]. Available: https://doi.org/10.1016/j.polymer.2018.12.057

[37] Y. Yuan, Y. Chen, W. L. Chen, and R. J. Hong, "Preparation, durability and thermostability of hydrophobic antireflective coatings for solar glass covers," *Sol. Energy*, vol. 118, pp. 222–231, Aug. 2015. [Online]. Available: https://doi.org/10.1016/j.solener.2015.04.044

[38] S. S. Latthe, S. Liu, C. Terashima, K. Nakata, and A. Fujishima, "Transparent, adherent, and photocatalytic SiO_2-TiO_2 coatings on polycarbonate for self-cleaning applications," *Coatings*, vol. 4, no. 1, pp. 497–507, Jul. 2014. [Online]. Available: https://doi.org/10.3390/coatings4030497

[39] J. Zhou *et al.*, "Preparation of transparent fluorocarbon/TiO_2-SiO_2 composite coating with improved self-cleaning performance and anti-aging property," *Appl. Surf. Sci.*, vol. 396, pp. 161–168, Feb. 2017. [Online]. Available: https://doi.org/10.1016/j.apsusc.2016.11.014

[40] N. Yu, X. Xiao, Z. Ye, and G. Pan, "Facile preparation of durable superhydrophobic coating with self-cleaning property," *Surf. Coatings Technol.*, vol. 347, pp. 199–208, Aug. 2018. [Online]. Available: https://doi.org/10.1016/j.surfcoat.2018.04.088